

# The Effects of Concentration, Pressure, and Temperature on the Diffusion Coefficient and Correlation Length of SDS Micelles

J. S. Collura,\* D. E. Harrison,<sup>†</sup> C. J. Richards,<sup>‡</sup> T. K. Kole,<sup>§</sup> and M. R. Fisch<sup>||</sup>

C–Squared, P.O. Box 630, Chagrin Falls, Ohio 44022

Received: December 20, 2000; In Final Form: March 15, 2001

The effects of sodium dodecyl sulfate (SDS) concentration ( $\leq 10$  mass %), temperature (35 and 50 °C), and pressure (0.1 to 100 MPa) on the cooperative diffusion coefficient and static correlation length of micelles in solutions in 1 M NaCl were studied using static and dynamic light scattering. These data are interpreted in terms of models of dilute and semidilute solutions of rod-like polymers. The results indicate that the effects of pressure are most significant near the crossover concentration between dilute and semidilute solution behavior. This concentration is a function of temperature and pressure because both of these thermodynamic parameters affect the mean micellar size.

## 1. Introduction

Aqueous solutions (often with added electrolytes) of many ionic surfactant molecules form long, flexible worm-like micelles.<sup>1,2</sup> The formation of these worm-like micelles depends, in a complex manner, on the intermolecular forces between the surfactant molecules, the solvent molecules, and the surfactant–solvent molecules.<sup>2,3</sup> In particular, this self-assembly also depends on the details of the surfactant molecule's molecular structure, such as the headgroup area, the length of the molecule and its volume, the molecule's net charge, the nature of the solvent and counterions, and the like.<sup>3</sup> From the viewpoint of external macroscopic variables, the thermodynamic conditions such as temperature, pressure, and concentration of both surfactant and additives are critical to the self-assembly and growth of these worm-like micelles. Thus, such systems can be understood and explained at many different levels. Correspondingly, a variety of experiments are needed to provide many different parameters.<sup>4</sup>

These micelles are in some ways similar to flexible linear polymers. The analogy between micelles and polymers and polyelectrolytes has recently been reviewed by Magid,<sup>5</sup> and while it is a useful starting point, it is not exact. In the simplest form of this analogy, which we will employ, the worm-like micelles will be treated as a polydisperse mixture of polymers of contour length,  $L$ , persistence length,  $l_p$ , and constant cross-sectional radius,  $r_{cs}$ . In the experiments described in this paper, the concentration of surfactant is significantly above the critical micelle concentration (CMC). Thus, the solvent will consist of water, ions, and monomers of surfactant. In contrast, the model assumes a pure solvent. For the solutions studied, the salt concentration is sufficiently high that, to a very good ap-

proximation, the intermicellar electrostatic interactions are negligible. For modest surfactant concentrations, those below the concentrations at which concentrated solution behavior or liquid crystals occur, the solution behavior of the micelles will then consist of two regimes, the dilute regime, and the semidilute regime.

The regime in which the concentration of micelles is sufficiently low that the micelles may be considered as very weakly interacting objects is called the dilute solution regime. Even in this regime, micellar growth can occur upon changing thermodynamic parameters and the surfactant concentration,  $C_D$ . The dependence of this growth on  $C_D$  is of particular interest and has been well studied.<sup>1,6</sup> In part, the reason for this interest is that the aggregation number distribution, and hence the mean micellar size, depends strongly upon the concentration of surfactant. Therefore, when the overall concentration of surfactant is increased, even when all other macroscopic variables are held constant, micellar growth occurs. There is also an increase in the number density of the micelles. The combination of these two effects leads to the formation of entangled transient networks of overlapping micelles. The overlap or crossover concentration  $C_D^*$  defines the onset of semidilute solution regime. The concentration at which this occurs is not a sharp point, but rather occurs over a range of concentrations. Despite this ambiguity, a good estimate of this concentration may be obtained experimentally.<sup>2,7,8</sup> This concentration is often of the order of a few percent or less by mass. Furthermore, it is a function of the mean contour length and the persistence length of the micelles. The mean contour length and persistence length of the micelles are a function of concentration of surfactant and other thermodynamic variables such as temperature, pressure, and concentration of counterions. Thus, one expects the crossover concentration to be a function of the same thermodynamic variables.

The study of how the physical properties of these solutions, including the mean contour and persistence lengths, depend on surfactant concentration and other thermodynamic variables has both intrinsic experimental and theoretical interest as well as practical use. For example, Carale and Blankschtein<sup>9</sup> have studied the effects of semidilute solution behavior on phase transitions in micellar systems. Ben-Shaul and Gelbart<sup>10</sup> have

\* To whom correspondence should be addressed. E-mail: Collura@IEEE.org

<sup>†</sup> Also Physics Department, Case Western Reserve University, Cleveland, OH 44106. Current address: Harrison Consulting, P.O. Box 198, Westmoreland, NY 13490.

<sup>‡</sup> Current address: Keithley Instruments, Inc., 28775 Aurora Road, Cleveland, OH 44139.

<sup>§</sup> Current address: Stanford Microdevices, 522 Almanor Ave., Sunnyvale, CA 94086.

<sup>||</sup> Current address: Liquid Crystal Institute, Kent State University, Kent, OH 44242.

noted that the growth laws, persistence lengths, and interaction parameters are all needed for further theoretical advancement in this area, and that more experimental data is needed. Semidilute solutions are common in many industrial products. Furthermore, there is great interest, both theoretical and experimental, in lyotropic nematic phases that are expected to form at even higher concentrations.

In this paper, we will present the results of static and dynamic light scattering studies of aqueous NaCl solutions of sodium dodecyl sulfate (SDS). The results indicate that the crossover concentration, in 1M NaCl, depends on temperature and pressure. Moreover, the characteristic sizes obtained from both dynamic and static light scattering depend on pressure and surfactant concentration, suggesting that the micellar shape is a function of pressure as well as concentration. SDS was chosen as the surfactant because it has been very extensively studied, both theoretically and experimentally.<sup>11</sup> In addition, in dilute solutions, the required molecular and thermodynamic parameters are well known.

## 2. Theory

The equilibrium properties of locally cylindrical linear micelles have been well studied.<sup>12</sup> It is important to observe that the theory described here has several limitations. It is valid only when the contour length of the worm-like micelles is much longer than the persistence length, it assumes only rod-like micelles exist (no branched or ring structures are included), and it is a mean-field approach. The effects of additional interactions are discussed in the literature.<sup>10</sup> In particular, a significant increase in the mean aggregation number can result from micellar interactions.

With these caveats in mind, theoretical predictions, in both the dilute and semidilute regimes, may be summarized as follows.<sup>13</sup> The number density of rod-like micelles of contour length,  $L$ , is given by

$$c(L) \propto \exp[-L/\bar{L}] \quad (1)$$

where the most probable contour length,  $\bar{L}$ , is given by

$$\bar{L} \propto \phi^b \exp[E/2k_B T] \quad (2)$$

In these expressions  $c(L)$  is the number density of chains as a function of the contour length,  $L$ . Further,  $\bar{L}$  is the most probable contour length and  $\phi$  is the volume fraction of surfactant (which is proportional to  $C_D$ ). The exponent  $b$  obtains a value of 0.5 in dilute solutions and approximately 0.6 in semidilute solutions. Finally,  $E$  is the scission energy of the chain (that is the energy required to create two new chain ends),  $k_B$  is the Boltzmann constant, and  $T$  is the absolute temperature. It is important to recall that, while SDS micelles are charged, the salt concentration in the present experiments is sufficiently high that the above results are not significantly changed by (long range) electrostatic repulsion.

The time fluctuations of the scattered light were analyzed using temporal autocorrelation. In this type of measurement, the normalized temporal intensity autocorrelation function,  $g_2(q, \tau)$  is determined. In the present experiment,  $g_2(q, \tau)$  is analyzed in terms of a cumulant expansion<sup>14</sup> and is expected to have the form

$$g_2(q, \tau) = \beta \exp[-2D_c q^2 \tau + F\tau^2 + \dots] + \text{background} \quad (3)$$

Here,  $\beta$  is an instrumental constant  $\leq 1$ ,  $D_c$  is the cooperative diffusion coefficient,  $q$  is the scattering vector

( $q = (4\pi n/\lambda)\sin(\theta/2)$ , where  $n$  is the index of refraction of the solution,  $\lambda$  is the vacuum wavelength of the incident laser light, and  $\theta$  is the scattering angle measured from the forward direction),  $F$  is a constant that can be related to the polydispersity of the particle size distribution, and *background* is the background term, which is normalized to 1. In very dilute solutions, where interparticle interactions can be ignored,  $D_c$  is identified with the free particle diffusion coefficient,  $D_0$ . This allows one to use the Stokes–Einstein relationship to obtain the mean hydrodynamic radius,  $R_H$ , of the micelles:<sup>15</sup>

$$R_H = \frac{k_B T}{6\pi\eta D_0} \quad (4)$$

where  $\eta$  is the shear viscosity of the solvent. It is important to note that  $R_H$  depends on both the micellar shape and size. In the semidilute solution regime, the same cumulant analysis can be performed and  $D_c$  obtained. However, in this solution regime one obtains the hydrodynamic correlation lengths,  $\xi_H$ .<sup>15</sup>

$$\xi_H = \frac{k_B T}{6\pi\eta D_c} \quad (5)$$

The physical interpretation of  $\xi_H$  is somewhat more complex than the hydrodynamic radius,  $R_H$ , or the static correlation length,  $\xi$ . For the present, it may be considered the size of a “vacancy” in the semidilute phase. In a semidilute polymer solution,  $D_c$  is predicted<sup>16</sup> to vary with the volume fraction of surfactant as

$$D_c \propto \phi^{.77} \quad (6)$$

The scattering vector or angular dependence of the mean scattered light intensity can be used to determine another characteristic size of the scattering objects. Once more, the analysis depends on the type of solution being analyzed. For dilute solutions, the mean scattered intensity as a function of scattering vector may be described by the Guinier form:<sup>17</sup>

$$I(q) = I_0 \exp\left[-\frac{q^2 \langle R_G^2 \rangle}{3}\right] \quad (7)$$

where  $I(q)$  is the mean scattered light intensity due to the scattering objects at scattering vector  $q$ ,  $I_0$  is the (extrapolated) scattered light intensity at  $q = 0$ , and  $\langle R_G^2 \rangle$  is the z-average squared radius of gyration of the micelles. It is important to note that  $\langle R_G^2 \rangle$  is the z-average square radius of gyration. Because it is an average over the micelle size distribution,  $c(L)$ , it generally does not correspond to the squared radius of gyration of a given micelle.  $R_G \equiv \sqrt{\langle R_G^2 \rangle}$  depends on micellar shape and size. For worm-like micelles (polymer chains) of contour length,  $L$ , and persistence length,  $l_p$ ,  $R_G^2$  has the following form:<sup>18</sup>

$$R_G^2(L, l_p) = (Ll_p/3) - l_p^2 + (2l_p^3/L) - (2l_p^4/L^2)(1 - \exp[-L/l_p]) \quad (8)$$

In this expression, the explicit contour length and persistence length dependence has been included in the argument of  $R_G^2$ .

The analysis of data obtained in the semidilute regime is once more different than that obtained in the dilute solution regime. In semidilute solutions the static correlation length,  $\xi$ , is determined from  $I(q)$ . In this case,  $I(q)$  is described by an Ornstein–Zernicke form

$$I(q) \propto \frac{1}{1 + q^2 \xi^2} \approx \exp[-q^2 \xi^2] \quad (9)$$

In the semidilute solution, a physical interpretation of  $\xi$  is to regard it as the distance between entanglements of the micelles.

The persistence length of the micelles may be obtained through equations that describe  $D_c(L, l_p)$  and  $\langle R_G^2 \rangle(L, l_p)$ . The first equation, based on the average diffusion coefficient, describes the dynamic size as a function of contour length and persistence length. The second will use  $\langle R_G^2 \rangle(L, l_p)$  to describe the static size as a function of the same variables. By use of these two equations, one should be able to determine the persistence length of the micelles. One particularly easy way to accomplish this in the dilute solution regime is to introduce<sup>19</sup> the parameter  $\rho$  that is defined as  $\rho \equiv R_G/R_{H0}$ , where  $R_{H0}$  is the hydrodynamic radius at  $q = 0$ . This quantity is a universal function of  $l_p$  and micellar diameter for given molecular parameters and size distribution.<sup>11</sup> In semidilute solutions the expression for this ratio becomes  $\rho = \xi/\xi_H$  which should equal one. Lastly, observe that we have introduced two correlation lengths,  $\xi$ , the static correlation length, and  $\xi_H$ , the hydrodynamic correlation length. Our data indicate that these two lengths are not the same over the part of the semidilute concentration range studied.

### 3. Experimental Details: Materials, Methods, and Equipment

**Materials.** The sodium dodecyl sulfate (SDS) was Fluka MicroSelect grade, the NaCl was from Fisher, and both were used without further purification. The water was from a Millipore Milli-Q water purification system and had a resistivity  $\geq 10$  MOhm cm.

**Sample Preparation.** The samples were prepared by dissolving the required mass of SDS in 10 mL of a 1-M solution of NaCl. Because dust could have been a problem in these light scattering experiments, the NaCl solutions were filtered through 0.2  $\mu$ m pore Anotop filters directly into the large scattering cells. Because room temperature is below or near the critical micellar temperature of these solutions, the samples were then sealed and heated to approximately 40 °C in a heating block and well mixed until a clear homogeneous sample was formed. Once this was completed, the sample was transferred to smaller scattering cells appropriate for the apparatuses used and centrifuged at 35 °C and 5500 rpm for one-half to 4 h. This helped ensure that any residual insoluble particles in the sample were on the inside wall of the sample cell out of the laser light path.

**Experimental Techniques.** Two different light scattering spectrometers were used for these experiments. The atmospheric pressure experiments were performed using a commercial Malvern 4700 light-scattering system. The relevant components of the instrument were a Lexel 95 Argon ion laser, temperature controlled index-matched scattering oven that controlled the temperature to  $\pm 0.1$  °C, 128-channel correlator, and a photomultiplier tube mounted on a goniometer. The whole system was computer controlled. The procedure for an atmospheric run consisted of placing the centrifuged sample into the light scattering oven and waiting for thermal equilibrium to be obtained. This typically occurred on the time scale of 10 min or less; nevertheless, at least 30 min were allowed before data was collected. The intensity autocorrelation function was determined at 12 scattering angles between 30 and 140 degrees in 10-degree steps. The mean scattered light was measured at these same angles or at 1-degree intervals between 10 and 138 degrees. Details are available elsewhere.<sup>20</sup>

The high-pressure light scattering apparatus is homemade and has been discussed elsewhere.<sup>21</sup> This instrument allowed us to measure the mean scattered light intensity and temporal autocorrelation function at five scattered angles, 45, 60, 90, 120, 135 degrees. The temperature control of this unit was better than  $\pm 0.05$  °C, and the pressure control generally significantly better than  $\pm 1$  MPa. These data were collected with a 64 channel Malvern autocorrelator. At atmospheric pressure, the diffusion coefficients determined with this apparatus were essentially the same as those determined using the Malvern 4700. Due to small irregularities in the goniometer of this instrument, the scattered intensities measured at one atmosphere using this instrument were corrected to yield the same characteristic size as that obtained with the Malvern 4700 instrument. This correction was only applied at the start of an experimental run. In this apparatus at least 30 min was also allowed for thermal equilibrium to be reached after changes in pressure. Details are discussed elsewhere.<sup>22</sup>

The data from both experiments were analyzed identically. The measured intensity autocorrelation function was fit using a nonlinear fitting routine to the theoretical form given in eq 3. From this fit the cooperative diffusion coefficient,  $D_c$ , was determined. The diffusion coefficients measured at each angle (or scattering vector,  $q$ ) and at constant temperature and pressure were then fit to a linear equation of the form

$$D(q) = D(q = 0) + Aq^2 \quad (10)$$

where  $A$  is a constant and  $D(q = 0)$  is the diffusion coefficient at zero scattering vector. This fitting procedure should largely eliminate the effects of internal modes and the like on the determined diffusion coefficient.<sup>19</sup> The  $D(q = 0)$ , or  $D(0)$  were then used with eq 4 or 5 to determine  $R_H(q = 0) = R_H(0) \equiv R_{H0}$  or  $\xi_H$ , depending upon the concentration. Recall that the concentration determines which type of solution behavior one is studying. Note, however, that near the crossover concentration the interpretation of the data as a length is not unique although a well-defined cooperative diffusion coefficient is experimentally determined. The mean scattered light intensity data were fit using a nonlinear least squares algorithm to eq 7 over the whole concentration regime. The resulting  $R_G$  were converted to  $\xi$  in the semidilute solution regime by noting from eqs 7 and 9 that  $\xi = R_G/\sqrt{3}$ . As noted by Fujita<sup>23</sup> and others,<sup>24,25</sup> this is strictly valid only at infinite dilution. The behavior of the correlation length has been studied in polymer solutions.<sup>24,25</sup>

### 4. Results

A major result is shown in Figure 1. This is a graph of the cooperative diffusion coefficient at zero scattering vector,  $D(0)$ , versus concentration at atmospheric pressure and 35 and 50 °C. The uncertainty in the fitted diffusion coefficient is typically 7%, and is smaller at higher concentrations. The minima of curves drawn through these data indicate the crossover concentration. Analysis of these curves indicates that the crossover concentration is approximately 1.5 mass % at 35 °C, and approximately 2.5 mass % at 50 °C. The increase in diffusion coefficient and increase in crossover concentration with increase in temperature is expected because the SDS micelles grow as the temperature is lowered. The solid lines through the data in the semidilute solution regime are power law fits, of the form  $D_c \propto (C_D)^x$ , a generalization to arbitrary exponent of eq 6. Here the mass fraction has been used rather than the volume fraction because the density of the SDS as a function of temperature is not known. The volume fraction is smaller than the mass



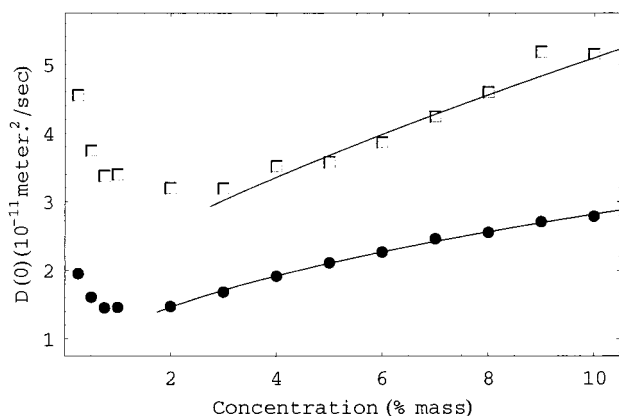


**Figure 1.** Cooperative diffusion coefficient versus concentration at 35° (lower curve) and 50° C (upper curve). The solid lines are least-squares fits to the form  $D_c \propto (C_D)^x$  for surfactant concentrations greater than the crossover concentration. The crossover concentration is the concentration at which  $D(0)$  obtains its minimum value. The values of  $x$  are discussed in the text.

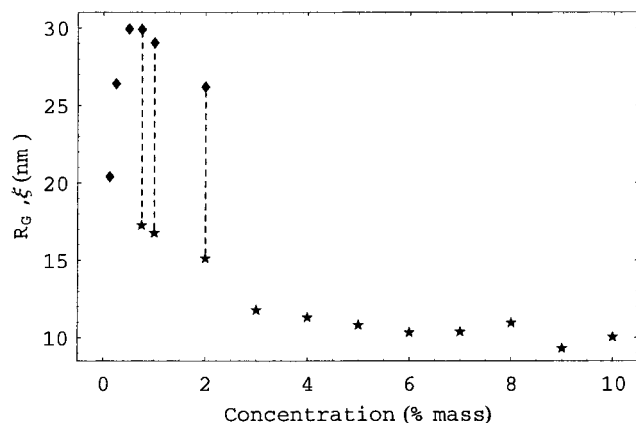


**Figure 2.** Characteristic size measured by static light scattering as a function of concentration of surfactant at 35° C. For  $C_D \leq 0.5\%$ , the characteristic length is the radius of gyration ( $\blacklozenge$ ). For  $C_D \geq 2\%$  the appropriate measure is the static correlation length ( $\star$ ). In the crossover region, neither measure has a clear physical meaning and these two measures are both shown with dashed lines between them.

fraction. However, the power,  $x$ , is rather insensitive to this difference at low concentrations. The exponent  $x$  obtains a value of 0.42 at 35 °C and 0.58 at 50 °C. This should be compared to the values 0.77 predicted theoretically and 0.81 measured in another surfactant system.<sup>26</sup> The prediction value assumes a very good solvent. Thus, this result also indicates that 1 M NaCl is not a particularly good solvent for SDS, and that it is a worse solvent at 35 °C than at 50 °C. This would seem to indicate that a condition for micellar growth is that the solvent be a “poor solvent.” While the diffusion coefficient is reported, the corresponding size, either  $R_H(0)$ , or  $\xi_H$  may then be obtained using either eq 4 or eq 5 as appropriate.

A second major result is the characteristic size obtained from static light scattering. Our instruments allowed us to measure this only at 35 °C. The angular variation in scattered light intensity is too small to be determined at 50 °C. Figure 2 is a graph of this characteristic length versus mass concentration at a pressure of 0.1 MPa and 35 °C. The fitting allows us to extract this length with an uncertainty of about 10%, except at the lowest concentrations where it is on occasion as large as 20%. There are three regions of interest in this graph. The first occurs at very low concentrations, and indicates increasing size with increasing concentration. This corresponds to the dilute solution

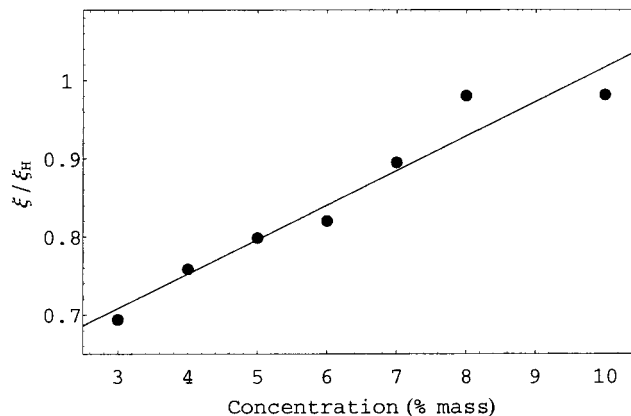


**Figure 3.** Ratio of the hydrodynamic to the static correlation length versus concentration at 35° C. All data are in the semidilute solution regime.

regime and includes concentrations less than about 0.5%. The size of interest in this region is the radius of gyration. The next region between roughly 0.75 and 2% corresponds to the ambiguous region where the micelles are beginning to strongly interact. This concentration region includes the crossover concentration,  $C_D^*$  and concentrations within a factor of 2 of this concentration. In this concentration region, it is difficult to apply a simple physical picture to the length scale measured. We have indicated this on the graph by showing both the mean radii of gyration,  $R_G$ , and the static correlation length,  $\xi$ . This is indicated by different symbols in the graph. The third region of interest corresponds to points with concentrations greater than approximately 3% and corresponds to semidilute solution behavior. In this region, there is a slight decrease in the static correlation length,  $\xi$ , with increasing concentration. It decreases from approximately 12 to 10 nm as the SDS concentration increases from 3% to 10%. Since  $\xi$  is roughly a measure of “pore size” in the solution, this indicates that the pore size decreases slightly over the greater than three-fold increase in concentration.

These two results may be combined. In the dilute solution regime, the resulting  $R_G/R_H(0)$  may be combined with theoretical models<sup>11,27</sup> for  $R_H(0)[L, l_p]$  to obtain estimates of the persistence length of the micelles. With only three concentrations, this was not pursued. Well into the semidilute regime, the corresponding quantity is  $\xi/\xi_H$ . This quantity is shown in Figure 3. Because this is a calculated quantity based on two numbers with uncertainty of 10% or less, the uncertainty of the calculated quantity may be as large as 15%. The important observation is that because this ratio is not one,  $\xi$  and  $\xi_H$  are not equal. At the lowest unambiguously semidilute solution that had a concentration of 3%,  $\xi/\xi_H$  obtains a value of 0.69, whereas at the highest concentration studied (10%) this ratio obtains a value of 0.98. This ratio is approximately a linear function of mass concentration in this region. It was extremely difficult to prepare samples with higher SDS concentration, so we did not extend this to higher concentrations. Well into the semidilute solution regime, these two quantities are expected to be identical.<sup>28</sup> The observed concentration dependence may be a manifestation of the (relatively) poor solvent properties of 1 M NaCl. In a poor solvent, a polymer chain tends to contract. For sufficiently poor solvent conditions a phase separation will occur.<sup>16</sup> In a situation where the concentration is increasing (and with this the intermicellar interactions) and the diffusing objects are getting smaller, it may be necessary to go well into the semidilute phase for equality of these two measures of size to occur. It may also

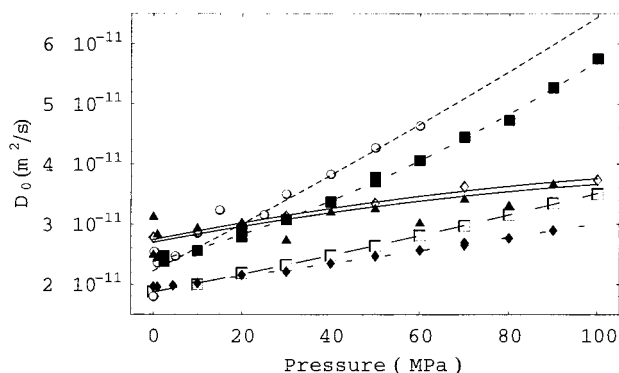


**Figure 4.** Diffusion coefficient as a function of pressure for five surfactant concentrations at 35 °C. The lines are least-squares fits that are discussed in the text [○: 0.5%, ■: 1%, □: 2%, ◆: 4%, ▲ and ◇: 8%].

be indicative of a more serious breakdown in the polymer–micelle analogy.

The concentration dependence of the two correlation lengths within the semidilute solution regime merits further discussion. It is important to realize that there are two static sizes in this problem. The first length is the correlation length,  $\xi$ , which characterizes the size of the blobs, or distance between entanglements of the micelles. The second is the radius of gyration,  $R_G$  which depends on the size and shape of the individual micelles and their distribution of sizes. It is generally understood that static light scattering determines  $R_G$  in dilute solutions and  $\xi$  in semidilute solutions. Further, there should be a continuous crossover from independent particle behavior to cooperative behavior. Also, in the semidilute solution regime, the dynamic light scattering equivalent to the hydrodynamic radius is the hydrodynamic correlation length,  $\xi_H$ , which is predicted to be the same as  $\xi$ . Thus, one interpretation of the results shown in Figure 3 is that despite these theoretical predictions  $\xi_H$  and  $\xi$  are not the same. This alternative is based on the observations that (a) the diffusion coefficient data is consistent with  $\xi_H \propto (C_D/C_D^*)^{-x}$  (with  $x = 0.58$ ), for  $C_D \geq C_D^*$ ; while (b) the static light scattering data should be a measure of  $\xi$ , and this measurement is substantially different from  $\xi_H$  except at the highest concentrations studied. An alternative interpretation is that the change in behavior of these two quantities occurs over somewhat different concentration regions. This would imply that the diffusion coefficient measured by dynamic light scattering experiments indicates crossover behavior at a lower concentration than the correlation length measured by static light scattering experiments. Thus, the static light scattering measurements are still in the dilute solution regime, but the crossover effects to semidilute solution behavior affect the values measured. By comparing our static light scattering results to the theory of Ohta and Nakanishi,<sup>25</sup> this possibility can be shown to be consistent with the data. A more careful experiment in which the correlation length, osmotic susceptibility, and diffusion coefficient are measured could help answer this question.

The effects of pressure on both the cooperative diffusion coefficient at zero scattering vector,  $D(0)$ , and the ratio of static to dynamic lengths are shown in Figures 4 and 5, respectively. Once more, the uncertainty in the plotted quantity is roughly 15% or less. The cooperative diffusion coefficient as a function of the concentration of SDS and pressure at  $T = 35$  °C is shown in Figure 4. At all five concentrations and all pressures studied, the effect of pressure is to increase  $D_c$ , or equivalently, within a given solution regime, decrease the mean size of the diffusing objects. This is true in both the dilute and the semidilute solution

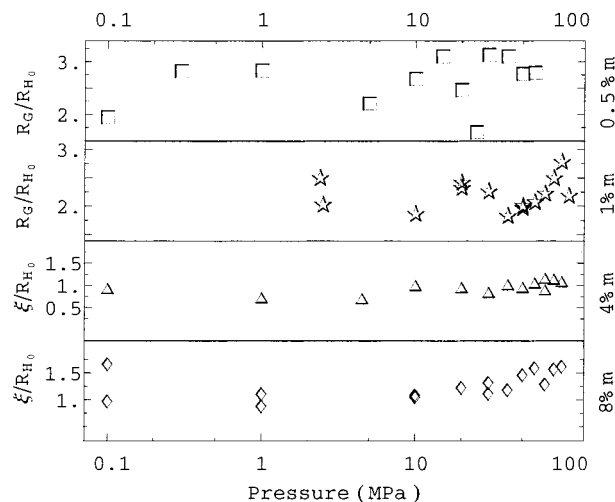


**Figure 5.** Ratio of static size to hydrodynamic size as a function of pressure for four concentrations. In dilute solutions the corresponding ratio is  $R_G/R_{H(0)}$ , whereas in semidilute solutions the corresponding ratio is  $\xi/R_{H(0)}$ . From top to bottom the panels correspond to 0.5%, 1%, 4%, 8% SDS.

**TABLE 1: Pressure Dependence of Mutual Diffusion Coefficient:  $D_0 = a + bP + cP^2$**

concentration SDS (%)	$a$ ( $10^{-11}$ m <sup>2</sup> /s)	$b$ ( $10^{-13}$ m <sup>2</sup> /s/MPa)	$c$ ( $10^{-16}$ m <sup>2</sup> /s/[MPa <sup>2</sup> ])
0.5	2.22	3.83	3.92
1	2.37	1.99	13.46
2	1.87	1.45	1.84
4	1.94	0.97	0.96
8	2.74	1.48	−4.67
8	2.69	1.42	−4.48

regimes. In both solution regimes, the rate of change of the cooperative diffusion coefficient is approximately linear with pressure. This was quantified by fitting the data to the following functional form:

$$D_0 = a + bP + cP^2 \quad (11)$$

All fits except that describing the functional form of the 1% SDS data were dominated by the linear term. The fits describing the 2 and 4% SDS data had a quadratic contribution that is roughly 10% of the linear contribution at the highest concentrations studied. At the maximum pressure, the 0.5 and 8% SDS samples exhibit a 30% contribution from the quadratic term. The 1% SDS sample has a quadratic contribution roughly equal to the linear contribution at the highest pressures studied. The rate of increase of cooperative diffusion coefficient with pressure is largest in the most dilute solution, 0.5% SDS where the slope is  $3.83 \times 10^{-13}$  m<sup>2</sup>/s-MPa. In the semidilute regime ( $C_D = 2, 4$  and 8%), the variation is essentially linear and the slope is substantially smaller, approximately  $1.4 \times 10^{-13}$  m<sup>2</sup>/s-MPa. The quadratic contribution is positive for concentration less than or equal to 4%, and negative for the 8% sample. These data are summarized in Table 1.

It is interesting to note that there is no apparent systematic variation in the pressure dependence of the diffusion coefficient or the ratio of static to dynamic sizes. We believe that this is a result of the fact that over the pressure range studied the solution does not change from dilute to semidilute solution behavior (or vice versa). Earlier experiments by Fisch and Benedek<sup>29</sup> indicate that at pressures not too far above those studied the critical micellar temperature of the solutions will be above the experimental temperature and the SDS will no longer form

micelles. At present, we have no model for the magnitude of these changes. However, the model of a semidilute solution as a solution with diffusing "blobs" of linear dimension  $\xi$  and isotropic compressibility does suggest that a power series in pressure would describe  $\partial V/\partial P|_T$  and, by symmetry, the variation of blob size with pressure. A significant result, consistent with the above observations, is that increased pressure causes an increase in the crossover concentration. For example, observe that at a pressure of 14 MPa,  $D_0$  of the 2% and 4% mass samples are identical. This would imply that at this pressure the crossover concentration has moved out to approximately 3%. From the data, the diffusion coefficient of the 2% sample and the 8% sample will be equal at a pressure near 110 MPa, just past the maximum pressure of the present apparatus. Thus, we anticipate that the crossover concentration will move to higher concentrations at even higher pressures.

The effects of pressure on the ratio of static scattering length and the hydrodynamic length are shown in Figure 5. This figure shows the ratio of these two lengths at 35° C and four concentrations: 0.5, 1, 4, and 8%, as a function of pressure. The top panel corresponds to a concentration of 0.5%, well in the dilute solution regime. Note that  $R_G/R_H(0)$  is essentially independent of pressure and obtains a value of approximately 2.8.<sup>11</sup> Such a large ratio is consistent with rod-like micelles or possibly even branched structures.<sup>11</sup> The noise in the data is the result of the smallness of both the radius of gyration and the hydrodynamic radius at the concentrations and pressures studied. The second panel shows the same quantity at a concentration of 1%, near, but at least at a pressure of one atmosphere below, the crossover concentration. At this concentration,  $R_G/R_H(0)$  is similar in magnitude to that observed in 0.5% solutions. However, between 30 and 100 MPa there appears to be a systematic increase in this ratio. This would indicate that at higher pressures the system is further from the crossover concentration—an observation consistent with the crossing of the  $D_0(P)$  curves. The next panel shows data for  $C_D = 4\%$ . Here, the effects of pressure are rather small; there may be a slight increase in  $\xi/\xi_H$  with pressure, but this quantity is generally  $\leq 1$  over the whole pressure range. Note that as pressure increases this concentration becomes closer to the crossover concentration. The last panel corresponds to  $C_D = 8\%$ , well into the semidilute solution behavior for all pressures studied. The important observation is that, at this concentration, increased pressure causes an increase in  $\xi/\xi_H$  and this quantity is very close to one. This is consistent with the two correlation lengths  $\xi$  and  $\xi_H$  being equal.

## 5. Summary

The concentration, temperature, and pressure behaviors of grown SDS micelles in 1 M aqueous solutions of NaCl has been measured. The effects of pressure on the semidilute solution behavior of this system and for many different surfactant concentrations have been measured for what we believe is the first time. The results, interpreted in terms of  $R_G/R_H(0)$ , confirm that at 35 °C dilute solutions contain rod-like micelles and these micelles remain rod-like for all pressures less than 100 MPa. The results indicate that under isothermal conditions an increase in pressure will cause an increase in the crossover concentration. While the evolution of the solution's behavior is continuous, this characteristic concentration roughly separates dilute solution behavior from semidilute solution behavior. A pressure of 70 MPa is sufficient to raise the crossover concentration from near 1.5% at 0.1 MPa to approximately 3%. Increased pressure appears to have very nearly the same effect on both the static

and dynamic correlation lengths measured well into the semidilute solution regime. This is consistent with the views of semidilute surfactant solutions adopted from polyelectrolytes and polymers, which treat these two lengths as equivalent. At the same time, the ratio of these two lengths is not constant throughout the semidilute phase. Close to the crossover concentration, this ratio obtains a value near 0.7, obtaining a value of 1 only for concentration nearly five times the crossover concentration. The effects of pressure are strongest on the cooperative diffusion coefficient of dilute solutions. The approximately linear increase of the cooperative diffusion coefficient with pressure in the semidilute solutions has a slope 5–6 times smaller than in dilute solutions, and is approximately independent of concentration. In this system, higher temperatures result in less micellar growth. Thus one expects, and it is confirmed, that the crossover concentration increases with increasing temperature. The crossover concentration is at a mass concentration of roughly 2.5% at 50° C and 1.5% at 35° C.

**Acknowledgment.** This work was supported by the National Science Foundation science and technology center: Advanced Liquid Crystal and Optic Materials Grant (ALCOM) grant No. DMR-8920147, and by the National Science Foundation under Grant No. DMR-9727708 to John Carroll University. This work was performed at the physics department of John Carroll University. The authors thank professors Harry C. Nash, Klaus Fritsch, and Graciella Lacueva for their support and useful comments.

## References and Notes

- (1) There is extensive literature. For example, see Porte, G.; Appel, J.; Poggi, J. *J. Phys. Chem.* **1980**, *84*, 3105, and Missel, P. J.; Mazer, N. A.; Benedek, G. B.; Young, C. Y.; Carey, M. C. *J. Phys. Chem.* **1980**, *84*, 1044.
- (2) *Micelles, Membranes, Microemulsions and Monolayers*; Gelbart, W. M., Ben-Shaul, A., Roux, D., Eds.; Springer: New York, 1994; chapters 1 and 2.
- (3) Reference 2, chapter 1, and Puvvada, S.; Blankschtein, D. *J. Phys. Chem.* **1989**, *93*, 1989.
- (4) A good older review is *Surfactant Solutions New Methods of Investigation*, Zana, R., Ed.; Marcel Dekker: New York, 1987. A recent example that combines the results of several techniques is Michels, B.; Watson, G. *J. Phys. Chem. B* **2000**, *104*, 228.
- (5) Magid, L. J. *J. Phys. Chem. B* **1998**, *102*, 4064, and references therein.
- (6) See for instance the second reference in ref 1, and Missel, P. J.; Mazer, N. A.; Carey, M. C.; Benedek, G. B. *J. Phys. Chem.* **1989**, *93*, 8354, and Missel, P. J.; Mazer, N. A.; Benedek, G. B.; Carey, M. C. *J. Phys. Chem.* **1983**, *87*, 1264.
- (7) Cates, M. E.; Candau, S. J. *J. Phys.: Condens. Matter* **1990**, *2*, 6869.
- (8) Kole, T. M.; Richards, C. J.; Fisch, M. R. *J. Phys. Chem.* **1994**, *98*, 4949.
- (9) Carale, T. R.; Blankschtein, D. *J. Phys. Chem.* **1992**, *96*, 459.
- (10) Reference 2, chapter 1.
- (11) See, for instance, refs 1 and 6 and Mishic, J. R.; Fisch, M. R. *J. Chem. Phys.* **1990**, *92*, 3222.
- (12) Once more, there is extensive literature. References 1 and 2 are good starting points, two other seminal references are: Mukerjee, P. *J. Phys. Chem.* **1972**, *76*, 5, and Israelachvili, J. N.; Mitchell, D. J.; Ninham, B. W. *J. Chem. Soc., Faraday Trans 2* **1976**, *72*, 1525.
- (13) This discussion follows the discussion of ref 7.
- (14) There are many references to this technique of analysis. The original theoretical work was by Koppel, D. E. *J. Chem. Phys.* **1972**, *57*, 4814. Our analysis was done using the analysis pack provided by Malvern Instruments and using the method discussed by Harrison, D.; Fisch, M. R. *Langmuir* **1996**, *12*, 6691.
- (15) Reference 2, chapter 2.
- (16) This is in several sources. A classic reference is de Gennes, P. G. *Scaling Concepts in Polymer Physics*; Cornell University Press: Ithaca, 1979; p 211.
- (17) Guinier, A.; Fournet, G. *Small Angle Scattering of X-rays*; Wiley: New York, 1956; pp. 126–133.

- (18) Yamakawa, H. *Modern Theory of Polymer Solutions*; Harper and Row: New York, 1971; p 56.
- (19) Light Scattering from Polymers, in *Advances in Polymer Science*; Burchard, W., Ed.; Springer-Verlag: Berlin, 1983; Vol. 48.
- (20) Kole, T. M. Masters Thesis, John Carroll University, 1994 (unpublished).
- (21) Richards, C. J.; Fisch, M. R. *Rev. Sci. Instrum.* **1994**, *65*, 335.
- (22) Richards, C. J. Masters Thesis, John Carroll University, 1994 (unpublished).
- (23) Fujita, H. *Polymer Solutions*; Elsevier: New York, 1990.
- (24) Wiltzius, P.; Haller, H. R.; Cannell, D. S.; Schaefer, D. W. *Phys. Rev. Lett.* **1983**, *51*, 1183.
- (25) Nakanishi, A.; Ohta, T. *J. Phys. A: Math Gen.* **1983**, *16*, 4155 and Ohta, T.; Nakanishi, A. *J. Phys. A: Math Gen.* **1985**, *18*, 127.
- (26) Candau, S. J.; Hirsdh, E.; Zana, R. *J. de Physique* **1984**, *45*, 1263.
- (27) Tsvetkov, V. N. *Rigid-Chain Polymers*; Consultants Bureau: New York, 1989; chapter 2.
- (28) Ref 23, p 200, and de Gennes, P. G. *Macromolecules* **1976**, *9*, 587 and 594.
- (29) Fisch, M. R.; Benedek, G. B. *J. Chem. Phys.* **1986**, *85*, 553.